**Atmospheric
Chemistry
and Physics**

Retrievals of chlorine chemistry kinetic parameters from Antarctic ClO microwave radiometer measurements

S. Kremser[1,8]**, R. Schofield**[2]**, G. E. Bodeker**[1,*]**, B. J. Connor**[3]**, M. Rex**[2]**, J. Barret**[4]**, T. Mooney**[4]**, R. J. Salawitch**[5]**,
T. Canty**[5]**, K. Frieler**[6]**, M. P. Chipperfield**[7]**, U. Langematz**[8]**, and W. Feng**[7]

[1]National Institute of Water and Atmospheric Research, Lauder, New Zealand
[2]Stiftung Alfred-Wegener Institut (AWI), Forschungsstelle Potsdam, Potsdam, Germany
[3]BC Consulting Ltd., Alexandra, New Zealand
[4]Stony Brook University, Stony Brook, New York, USA
[5]Department Atmosphere & Ocean Science, University of Maryland, Maryland, USA
[6]Potsdam Institute for Climate Impact Research (PIK), Potsdam, Germany
[7]Institute for Climate & Atmospheric Science, School of Earth & Environment, University of Leeds, Leeds, UK
[8]Freie Universität Berlin, Berlin, Germany
[*]now at: Bodeker Scientific, Alexandra, New Zealand

Abstract. Key kinetic parameters governing the partitioning of chlorine species in the Antarctic polar stratosphere were retrieved from 28 days of chlorine monoxide (ClO) microwave radiometer measurements made during the late winter/early spring of 2005 at Scott Base (77.85° S, 166.75° E). During day-time the loss of the ClO dimer chlorine peroxide (ClOOCl) occurs mainly by photolysis. Some time after sunrise, a photochemical equilibrium is established and the ClO/ClOOCl partitioning is determined by the ratio of the photolysis frequency, J, and the dimer formation rate, k_f. The values of J and k_f from laboratory studies remain uncertain to a considerable extent, and as a complement to these ongoing studies, the goal of this work is to provide a constraint on that uncertainty based on observations of ClO profiles in the Antarctic. First an optimal estimation technique was used to derive J/k_f ratios for a range of K_{eq} values. The optimal estimation forward model was a photochemical box model that takes J, k_f, and K_{eq} as inputs, together with a priori profiles of activated chlorine ($ClO_x = ClO + 2 \times ClOOCl$), profiles of ozone, temperature, and pressure. JPL06 kinetics are used as a priori in the optimal estimation and for all other chemistry in the forward model. Using the more recent JPL09 kinetics results in insignificant differences in the retrieved value of J/k_f. A complementary approach was used
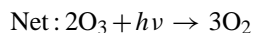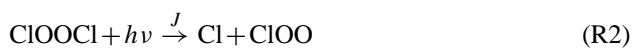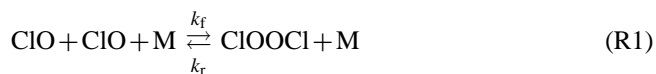
to derive the optimal kinetic parameters; the full parameter space of J, k_f, K_{eq} and ClO_x was sampled to find the minimum in differences between measured and modelled ClO profiles. Furthermore, values of K_{eq} up to 2.0 times larger than recommended by JPL06 were explored to test the sensitivity of the J/k_f ratio to changes in K_{eq}. The results show that the retrieved J/k_f ratios bracket the range of 1.23 to 1.97 times the J/k_f value recommended by JPL06 over the range of K_{eq} values considered. The retrieved J/k_f ratios lie in the lower half of the large uncertainty range of J/k_f recommended by JPL06 and towards the upper portion of the smaller uncertainty range recommended by JPL09.

1 Introduction

The photochemistry of the chlorine monoxide dimer, chlorine peroxide (ClOOCl; hereafter "the dimer") in the polar stratosphere is central to quantitatively describing polar ozone depletion and hence the Antarctic ozone hole. The formation and photolysis of ClOOCl, known as the ClO dimer cycle (Molina and Molina, 1987), is typically responsible for 55% to 70% of the spring-time ozone depletion in the Antarctic stratosphere (Frieler et al., 2006; SPARC, 2009). When high chlorine monoxide (ClO) concentrations are present in the polar stratosphere, the ClO dimer cycle:

$$ClO + ClO + M \underset{k_r}{\overset{k_f}{\rightleftharpoons}} ClOOCl + M \qquad (R1)$$

$$ClOOCl + h\nu \overset{J}{\rightarrow} Cl + ClOO \qquad (R2)$$

$$ClOO + M \rightarrow Cl + O_2 + M \qquad (R3)$$

$$2 \times [Cl + O_3 \rightarrow ClO + O_2] \qquad (R4)$$

$$Net : 2O_3 + h\nu \rightarrow 3O_2$$

becomes an extremely efficient ozone loss process. The terms k_f and k_r refer to the reaction rate constants for the formation and the thermal dissociation of the dimer, respectively. M represents any molecule to remove excess energy and J is the photolysis frequency of the dimer, which is directly related to the dimer absorption cross-section. Reactions (R2) and (R3) are the most important for ozone destruction since they release chlorine (Cl) atoms that then react with ozone (Reaction R4). Reaction (R2) is the rate limiting step for loss of ozone in the cycle.

If ClOOCl decomposes thermally (Reaction R1) rather than being photolysed (Reaction R2), or if the photolysis reaction produces ClO, a null cycle results that leads to no change in ozone. During day-time ClOOCl loss occurs mainly by photolysis and the partitioning between ClO and ClOOCl, as well as the overall rate of the catalytic cycle, are controlled by the dimer formation rate (k_f) and photolysis frequency (J). When sufficient time has passed after sunrise, the reaction system reaches a photochemical steady state, and the partitioning between ClO and ClOOCl is given by the expression:

$$\frac{[ClO]^2}{[ClOOCl]} \sim \frac{J}{k_f[M]} \qquad (1)$$

During night-time the temperature dependent thermal equilibrium constant K_{eq} governs the partitioning between ClO and ClOOCl:

$$K_{eq} = \frac{k_f}{k_r} = \frac{[ClOOCl]}{[ClO]^2} \qquad (2)$$

Uncertainties in these kinetic parameters (J, k_f and K_{eq}) contribute to differences between measured and modelled polar stratospheric ClO (e.g., Stimpfle et al., 2004), affect our ability to accurately describe polar ozone destruction (e.g., Frieler et al., 2006; von Hobe et al., 2007), and our ability to confidently project the response of polar ozone to future changes in stratospheric chlorine loading (e.g., SPARC, 2009).

Models of polar ozone photochemistry have traditionally used values of the ClOOCl absorption cross-section and k_f recommended either by the JPL data panel (e.g., Sander et al., 2003, 2006, 2009) or the IUPAC Subcommittee on Gas Kinetic Data Evaluation panel (Atkinson et al., 2007). Values of the ClOOCl cross-section recommended by the various panels typically fell between laboratory measurements by Huder and DeMore (1995) (low range in photolytically

active region) and Burkholder et al. (1990) (high range). In 2007, Pope et al. published ClOOCl absorption cross-sections that were considerably lower than either the Sander et al. (2006) (hereafter: JPL06) or Atkinson et al. (2007) recommendations. This lower photolysis frequency would make it impossible to quantitatively explain observed ozone loss with known chemistry, suggesting that as yet unknown processes were active. More recent laboratory studies by von Hobe et al. (2009), Chen et al. (2009), Papanastasiou et al. (2009), and Wilmouth et al. (2009) concluded that the correction applied by Pope et al. to account for Cl_2 contamination in their ClOOCl sample may have been too large. This in turn would lead to cross-sections which are too small in the atmospherically important wavelength region (>300nm). That said, these studies published in 2009 do not agree on the absorption cross-sections for the dimer, and so there remains uncertainty on the photolysis frequency for the ClO dimer. Comparisons between measured and modelled ClO (von Hobe et al., 2007; Schofield et al., 2008) concluded that no combination of k_f and K_{eq} was compatible with the absorption cross-sections measured by Pope et al. (2007).

Furthermore, field measurements of ClO and ClOOCl by von Hobe et al. (2007) and Stimpfle et al. (2004) and satellite measurements of ClO by Santee et al. (2010) indicate discrepancies in the equilibrium constant K_{eq} for ClOOCl compared to the JPL06 recommendation, and the more recent JPL09 recommendation. Therefore, there is a need to reduce the uncertainties in these reaction kinetic parameters, and thereby reduce uncertainties in modelled polar ozone loss.

In this study, two methods, both using ClO microwave radiometer measurements from Scott Base (78.85° S, 166.75° E), Antarctica, during the late winter and early spring of 2005 (described in Sect. 2), are used to constrain the kinetic parameters governing ClO chemistry in the polar stratosphere, viz.:

1. An optimal estimation approach (Sect. 3), using a photochemical box model as a forward model, is used to derive optimal J/k_f ratios consistent with the measured ClO profiles.

2. An exploration of the J, k_f, K_{eq} and ClO_x ($ClO_x = ClO + 2 \times ClOOCl$, i.e. active chlorine) parameter space, within physically plausible limits, to find where the minimum of measurement-model differences occurs.

The first approach is significantly faster than the second and provides statistical uncertainties on the derived parameters. The second, in addition to showing which set of parameters minimizes the measurement-model difference, also shows the regions within the 4D-space (4 dimensions, i.e. J, k_f, K_{eq}, and ClO_x) where differences of a similar magnitude are obtained. The second method also shows whether there are local minima in the 4-D-space that might provide a set of

viable kinetic parameters consistent with the field observations. The results obtained are presented and compared with previously published results in Sect. 4. These results are discussed in Sect. 5, followed by the conclusion of this study in Sect. 6.

2 Observations and model data

2.1 Observations

Stony Brook University and National Institute of Water and Atmospheric research (NIWA) have jointly operated a ground-based ClO microwave radiometer at Scott Base, Antarctica, since February 1996. The instrument and the ClO measurements are described in more detail in Solomon et al. (2000) and Connor et al. (2007). Briefly, the microwave radiometer measures the thermally-excited emission of ClO at 278.6 GHz within a frequency band of 506 MHz. As the ClO molecule has a very weak line amplitude, it is necessary to integrate the measured signals over some time period. Therefore, to generate the day-time and night-time ClO spectra, the individual ClO spectra, measured in 20 min time intervals, are averaged over the day-time and night-time period, respectively. Day-time is defined as 3 h after sunrise until 1 h before sunset at 20 km altitude, while night-time is defined as 4 h after sunset until 1 h before sunrise at 20 km altitude. The sunset and sunrise at 20 km altitude is defined by a solar zenith angle of 94.5°. An ozone line within the ClO microwave emission band interferes with the measurement. To eliminate this interference, and instrumental artefacts, the day minus night ClO spectrum is obtained by subtracting the mean night-time spectrum from the mean day-time spectrum. At night, Reaction (R1) dominates Reaction (R2), leading to most ClO_x being in the form of ClOOCl and, as a result, depending on the day of the year, night-time ClO is less than ∼20% of day-time ClO. The day minus night subtraction is essential for the analysis of the measured spectra to remove the ozone line and artefacts. The day minus night definitions were determined by detailed examination of spectra intensity relative to sunrise and sunset and the definition for day and night was chosen so that periods where ClO changes rapidly were avoided (Solomon et al., 2002).

ClO profiles from 10 to 56 km are derived from the ClO day minus night spectra. It should be noted that although the vertical resolution of the retrieved ClO profile is about 10 km, the location of the peak in the ClO mixing ratio can be determined to an accuracy of 1 to 2 km (Solomon et al., 2000, 2006). Retrieved concentrations of ClO on 20 altitude levels from 11 to 30 km are used in this analysis because ClO reaches its maximum abundance within this range of altitude. Twenty-eight days of ClO profiles, made during the period from 21 August to 20 September 2005 (Fig. 1), are used in this study, as 2005 offered the most comprehensive dataset. Due to bad weather conditions there were no ClO measure-
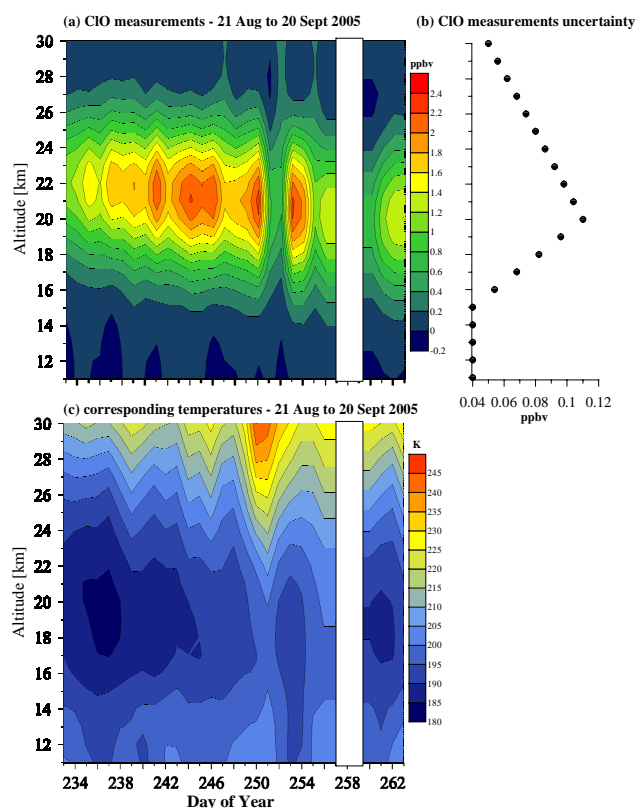

Fig. 1. Measured ClO concentrations in ppbv (panel **a**), the corresponding errors (panel **b**) and the coincident temperatures in K (panel **c**) plotted as a function of altitude and day of the year in 2005. The blue and organge/red colours in panel **(a)** depict low ClO concentrations (below 0.2 ppbv) and high ClO concentrations (above 1.6 ppbv), respectively. In panel **(c)**, low temperatures (below 210 K) are indicated by the blue colour range, while high temperatures (above 225 K) are shown in the yellow to red colour scale. There are no ClO measurements available for the period of 14–16 September 2005 (day 257 to 259) due to bad weather conditions (white bar).

ments available from 14–16 September 2005 and therefore these days are not considered in this study. At the beginning of the season (late August) the peak ClO mixing ratio occurs at around 22 km. In early September the peak ClO mixing ratio shifts downwards, occurring at 20–21 km. The maximum ClO mixing ratio increases from 1.2 parts per billion by volume (ppbv) to 2.3 ppbv within the 28 day period. Between 17 and 23 km the temperatures reach their seasonal minimum (<190 K) during this time period, as also shown in Fig. 1. The atmospheric temperatures shown in Fig. 1 were extracted for the location of Scott Base from the National Centers for Environmental Prediction, NCEP (Kalnay et al., 1996) reanalyses using bilinear interpolation.

2.2 Model output – SLIMCAT 3-D CTM

Output from the SLIMCAT 3-D off-line chemical transport model was used to provide estimates of the abundance of active chlorine ($ClO_x = ClO + 2 \times ClOOCl$), active bromine ($BrO_x = BrO + BrCl$), and ozone over Antarctica. The model is described in detail in Chipperfield (1999, 2006). Briefly, SLIMCAT contains a detailed stratospheric chemistry scheme, including heterogeneous reactions of liquid and solid polar stratospheric clouds (PSCs). The model uses a limited number of small families in the chemistry module. Chlorine (Cl), ClO and ClOOCl form a family and the partitioning between these species is found assuming instantaneous photochemical equilibrium. All other inorganic chlorine species (e.g. chlorine dioxide (OClO), hypochlorous acid (HOCl) etc.) are integrated separately. Similarly bromine (Br) and bromine monoxide (BrO) are solved as a family while all other inorganic bromine species are integrated separately (e.g. bromine monochloride (BrCl)).

For this study output was taken from the SLIMCAT 3-D CTM. The run used here (for reference, run 509) has a resolution of $5.6° \times 5.6°$ with 32 levels from the surface to about 60 km and was started on 1 January 1977. The run was forced using European Centre for Medium-Range Weather Forecasts (ECMWF) analyses (ERA-Interim after 1989). Daily profile output from the model run was stored for the location of Scott Base. The run included a source of bromine from very short-lived species, which contributed about 6 parts per trillion by volume (pptv) to total stratospheric inorganic bromine (Br_y) in 2005 (Feng et al., 2007).

3 Retrieval algorithm/optimal estimation

An optimal estimation (OE) approach (Rodgers, 2000) is used to retrieve the kinetic parameters that optimize the agreement between the measured ClO profiles and profiles generated by the OE forward model. The quantities to be retrieved, J/k_f and ClO_x, from the ClO measurements (Y) are represented, together with K_{eq} and a dataset of 28 a priori ClO_x profiles, by the state vector (X). The resulting state vector has 563 elements, 3 kinetic parameters plus 28 days $\times$ 20 altitudes for a priori ClO_x. Rather than working with J/k_f and K_{eq} explicitly, they are specified as scalings (multiplicative factors) relative to the JPL06 recommendations. Hereafter, all quantities subscripted with scale refer to scaling with respect to JPL06. JPL06 kinetics are the point of reference for this study because these kinetic parameters are most commonly used in recently published studies of polar ozone photochemistry. In some cases, results are also compared with the more recent JPL09 recommendation. The JPL09 K_{eq} value is $\sim 70\%$ of the JPL06 value, while J/k_f for JPL09 shows essentially no difference from JPL06, except for a reduction of the uncertainties.

The relationship between the ClO measurements (Y) and the state vector is described by a forward model (F) that calculates ClO as a function of the state vector X and other parameters, b, which include BrO_x, ozone, temperature, and pressure profiles:

$$Y = F(X, b) + \varepsilon \tag{3}$$

where ε is the measurement error. The error analysis for the Antarctic ClO measurements used in this study is described in depth in Solomon et al. (2000). The forward model (F) is a photochemical steady state box model, based on polar ozone photochemistry and described in detail by Salawitch et al. (1993). The Salawitch et al. box model is used to calculate ClO at 30 min resolution for the 28 day period considered, for various specifications of the kinetic parameters, which are set to JPL06 values if not otherwise noted. Daily day minus night ClO profiles, hereafter modelled ClO ($\hat{Y}$), are calculated from the 30 min time resolution output of the box model using the same definition of day and night-time as for the analysis of the ClO measurements, to provide compatibility with the measured ClO profiles. For b, the daily BrO_x profiles were obtained from the SLIMCAT 3-D CTM (see Sect. 2.2). Because vertical ozone profiles from ozonesondes were not available for each day of the analysis period, ozone profiles were extracted from the SLIMCAT simulation. Linearly interpolated differences between measured and modelled ozone profiles were added to the SLIMCAT profiles so that they matched the ozonesonde measurements (taken from Hassler et al., 2008) on the days when measurements were available and provided best-estimates of ozone profiles on intervening days. Similar to the temperature profiles (Sect. 2.1), the pressure profiles for the analysis period were extracted from the NCEP reanalyses.

The inverse of Eq. (3) produces X as an output for a given Y. There is an infinite set of such state vectors X that could form solutions to Eq. (3), reproducing the prescribed measurements. The retrieval problem is said to be under constrained, as there are more elements in the state vector than there are measurements. Given an a priori state vector (X_a), uncertainties on the elements of X_a (the covariance matrix S_a) and the measurement error, the OE retrieves an optimal state vector ($\hat{X}$) that minimizes the difference between measured and modelled ClO. X_a constrains the OE algorithm. The iterative equation for the solution of the inverse of Eq. (3) is:

$$\hat{X}_{i+1} = X_a + (S_a^{-1} + K_i^T S_e^{-1} K_i)^{-1} K_i^T S_e^{-1} \cdot [Y - F(\hat{X}_i) \tag{4}$$
$$+ K_i(\hat{X}_i - X_a)]$$

where K is the weighting function matrix, with each element representing the partial derivative of the modelled ClO with respect to a state vector element; i.e. $K_{ij} = dF_i(X)/dX_j$. As such, the weighting functions describe the sensitivity of the modelled ClO to variations in the state vector and were determined by consecutively perturbing each state vector quantity and recalculating ClO using the forward model. S_e in
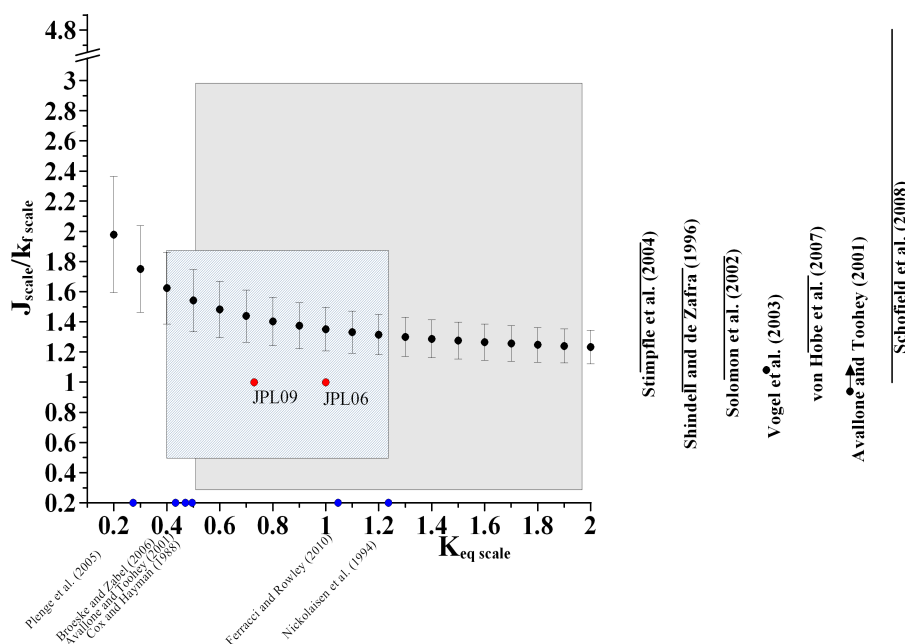
Fig. 2. The retrieved scale factors and 1σ uncertainties for J/k_f and K_{eq} from all OE runs. Vertical bars along the y-Axis: Results from earlier studies for $J_{scale}/k_{f\ scale}$ at 190 K. Blue symbols along the X-axis: $K_{eq\ scale}$ relative to JPL06 determined from earlier studies ($190 < T < 210$ K). Light grey area: JPL06 uncertainty range on K_{eq} and J/k_f. Smaller rectangular hatched area towards the bottom left: JPL09 uncertainty range on K_{eq} and J/k_f (for more details see text).

Eq. (4) is the covariance matrix of the measurement errors (Fig. 1b), constructed by placing the ClO measurement errors along the diagonal, and set to zero everywhere else. X_a was constructed by inserting values for $k_{f\ scale}$, $K_{eq\ scale}$ and J_{scale}, all set to 1.0 so that the a priori for the kinetics are the JPL06 recommendations. A set of 28 a priori ClO_x profiles, corresponding to each day of measurement, is provided as a required input to the forward model.

The uncertainties on the elements of X_a are expressed along the diagonal of a covariance matrix S_a, which is elsewhere set to zero. Selection of the S_a settings requires some subjective judgement, noting that if excessively small values are chosen, the retrieval will be constrained too tightly. In this case the retrieval will make little use of the information provided by the measurements and will differ little from the prescribed a priori X_a. On the other hand, if excessively large values for S_a are chosen, this results in an unrealistic retrieval where the measurement noise is interpreted as information. Here the S_a values for $k_{f\ scale}$, J_{scale} and the a priori ClO_x profiles were numerically determined as described in Schofield et al. (2004) and are set to $\sigma_{k_{f\ scale}} = 0.043$ and $\sigma_{J_{scale}} = 0.173$. The S_a values for the a priori ClO_x were set to 20 % of the daily maximum ClO_x value, individually for each day, also as done by Schofield et al. (2004).

During day-time the partitioning of ClO and its dimer is governed by J/k_f (see Eq. 1). K_{eq} becomes important primarily for the night-time partitioning of ClO_x. Because the night-time spectrum was subtracted from the day-

time spectrum to obtain a daily measured ClO profile, the ClO measurements mostly give information on J/k_f, and only very little information on these parameters individually. Furthermore, the measurements are only weakly sensitive to K_{eq}. Therefore, with the OE approach we retrieve $J_{scale}/k_{f\ scale}$ and make no attempt to retrieve K_{eq}. Rather, to test the sensitivity of our results to the choice of $K_{eq\ scale}$, OE is done 19 times, varying $K_{eq\ scale}$ from $0.2 \times K_{eq\ JPL06}$ to $2.0 \times K_{eq\ JPL06}$ in steps of $0.1 \times K_{eq\ JPL06}$.

Complementary to the OE approach, a second method was used to derive the kinetic parameters of the ClO dimer cycle. In this approach the full parameter space was explored by varying the values of the J, k_f and $K_{eq\ scale}$ factors within physically plausible ranges. Furthermore, to estimate the dependence of the retrieved kinetic parameters on changes in the prescribed ClO_x profile, the ClO_x profile was scaled between 0.5 and 1.0 times the a priori ClO_x profile used in the OE approach, in steps of 0.1 times the a priori ClO_x profile (scalings above 1.0 were not used since this resulted in ClO_x occasionally exceeding the total stratospheric inorganic chlorine (Cl_y) loading). The photochemical model described above in Sect. 3 was also used here, with the same input variables (i.e. BrO_x, ozone) to calculate day minus night profiles of ClO (again, to be compatible with the ClO measurements). The kinetic values that give the smallest difference between the modelled and the measured ClO are compared to the results from the OE and previous publications.

4 Results

4.1 Retrieved kinetic parameters from optimal estimation

The measurements were well described by the forward model for each OE run, with root mean square (RMS) differences between measured and modelled ClO ranging from 0.063 to 0.066 ppbv, which is smaller than the maximum error of the ClO measurements (0.11 ppbv). The results from the retrievals performed as outlined in Sect. 3, expressed as scale factors relative to the kinetic parameters recommended by JPL06, are shown together with 1σ uncertainties in Fig. 2. In addition to prescribing J and k_f from JPL06 as a priori in the forward model, JPL06 kinetics were used for all other chemistry in the forward model. The derived RMS values for the 19 OE runs do not vary much (only by $\sim 5\%$), but the change in the retrieved J/k_f ratios over the prescribed K_{eq} range (0.2 to 2.0) is significant. The ratio retrieved by prescribing $K_{eq\ scale} = 2.0$ is about a factor of 1.6 smaller than the $J_{scale}/k_{f\ scale}$ ratio retrieved for the smallest $K_{eq\ scale} = 0.2$ used in this study. Tests using JPL09 kinetics showed only very slightly ($\sim 2\%$) larger values for the $J_{scale}/k_{f\ scale}$ ratio, which is an insignificant difference given other sources of uncertainty. A $J_{scale}/k_{f\ scale}$ value of 1.0 refers to the JPL06 recommendations, where the photolysis frequency of the dimer (J) is calculated using the absorption cross-sections recommended JPL06. $J_{scale}/k_{f\ scale}$ values relative to JPL06 determined in earlier studies are indicated with vertical bars along the Y-axis in Fig. 2. The salient features of Fig. 2 and their causes are:

- Negative slope: When prescribing K_{eq}, according to Eq. (2), the night-time partitioning between ClO and its dimer and therefore night-time ClO concentrations are prescribed in the forward model, with larger K_{eq} meaning lower night-time ClO concentrations. As a result, depending on the choice of K_{eq}, different modelled night-time ClO concentrations were subtracted from the modelled day-time ClO concentrations to calculate the day minus night profile, which is compared to the ClO observations. When trying to minimize the differences between modelled and observed profiles, optimal estimation compensates for the differences in the modelled day minus night ClO profiles resulting from different choices of $K_{eq\ scale}$ by varying $J_{scale}/k_{f\ scale}$. Therefore, optimal estimation increases $J_{scale}/k_{f\ scale}$ for smaller $K_{eq\ scale}$, resulting in more ClO during the day (see Reactions R1, R2).

- Asymptotic behaviour of $J_{scale}/k_{f\ scale}$ at high $K_{eq\ scale}$: At K_{eq} values greater than $1.2 \times K_{eq\ JPL06}$ night-time ClO concentrations become almost negligible so that the modelled day minus night ClO profiles are rather similar and the retrieved optimal $J_{scale}/k_{f\ scale}$ values do not vary significantly.

Due to the lack of ClO night-time measurements it is not possible to determine the exact K_{eq} that corresponds to the Antarctic ClO measurements made during the analysis period. Therefore, in this study, a single value for J/k_f that best reproduces the measurements also cannot be determined, but rather a range of J/k_f values is provided depending on the choice of K_{eq}.

The $J_{scale}/k_{f\ scale}$ ratio of 1.39 interpolated to the K_{eq} prescribed by Solomon et al. (2000) ($K_{eq\ scale} = 0.86$) agrees very well with their $J_{scale}/k_{f\ scale}$ ratio (see Fig. 2). Solomon et al. used measurements from the same ClO microwave radiometer at the same site. The measurements they used were taken from a different period (late winter/early spring 1996–2000) when when stratospheric temperatures were, on average, 4 K lower than in the analysis period our study focuses on, i.e. the period from 21 August to 20 September 2005 (Fig. 1c). The formation rate of the dimer and the equilibrium constant are both known to be temperature dependent. A decrease in temperature leads to an increase in the dimer formation rate k_f, which in turn leads to a decrease in the J/k_f ratio. However, Solomon et al. used the JPL97 functional form for the temperature dependence of k_f, which is different from the JPL06 expression used here. The difference between JPL97 and JPL06 then partially offsets the effect of the temperature difference between the two studies.

The retrieved $J_{scale}/k_{f\ scale}$ ratios from all 19 OE runs lie within the lower half of the large uncertainty range given by JPL06, within the upper half of the smaller uncertainty range given by JPL09, and with most of the $J_{scale}/k_{f\ scale}$ ratios determined in previous studies (Fig. 2). The results suggest that to explain the ClO measurements measurements from Scott Base, Antarctica, made from August to September in 2005, J/k_f is unlikely to be smaller than the JPL06/09 recommendations. This result would exclude the lower uncertainty limit on J/k_f for both JPL06 and JPL09.

The best fit to the ClO measurements, i.e. the smallest RMS of the difference between modelled and measured ClO, is obtained at $K_{eq\ scale} = 2.0$. In this case $J_{scale}/k_{f\ scale}$ is 1.23 ± 0.11. In contrast to previous studies, our results suggest that to best represent the ClO measurements, $K_{eq\ scale}$ must lie towards the upper end of the prescribed range (0.2 to 2.0), in agreement with the recent laboratory study of Ferracci and Rowley (2010). However, the derived K_{eq} values in Ferracci and Rowley were obtained at higher temperatures than in this study. To explain the ClO measurements, the results presented in this study (Fig. 2) do not preclude higher K_{eq} values than currently recommended. That said, the decrease in RMS from $K_{eq\ scale} = 0.2$ to 2.0 is small (5 %), suggesting that K_{eq} is not well constrained by the measurements of ClO and therefore a robust evaluation of K_{eq} is difficult (see Sect. 3).

The RMS values obtained from the OE are elevated as a result of the inclusion of two days of measurements. Between 7 September (day 250) and 8 September 2005 (day 251), ClO dropped from ~ 2.2 ppbv to ~ 0.8 ppbv before increasing

back to $\sim$2 ppbv two days later (see Fig. 1a). The suppressed values of ClO over this two day period are caused by dynamical variability of the polar vortex. While SLIMCAT shows some reduction in ClO_x over this period, the reduction is not commensurate with the observed reduction in ClO, as is apparent in the disagreement between measured and SLIMCAT modelled ClO profiles on these days (not shown). With the given resolution of the SLIMCAT run (see Sect. 2.2), the model cannot capture the observed strong gradients at the edge of the vortex. Therefore, the a priori ClO_x profiles provided by SLIMCAT are too high on those two days. The value of $J_{scale}/k_{f\ scale}$ is determined by the partitioning of ClO and ClOOCl on all days and is not determined separately for every day. The amount of ClO_x, on the other hand, can vary for every day independently within the given uncertainty range, which is determined by the set up of the a priori uncertainty ($\mathbf{S}_a$). The selection of the magnitude of the elements of $\mathbf{S}_a$ determines the freedom of the OE, i.e. how well constrained is the OE. The selected uncertainties on the a priori ClO_x profile (see Sect. 3) are likely to be too small for the two days and therefore the OE is constrained too tightly. The retrieval does not have enough freedom to modulate ClO_x, for the given $J_{scale}/k_{f\ scale}$, to reproduce the measurements. The combination of $J_{scale}/k_{f\ scale}$ with a higher amount of ClO_x leads to more ClO than observed and thereby contributes to the higher RMS values. While excluding the two days from the analysis reduces the RMS such that it is smaller than the measurement uncertainty at every altitude level, the retrieved $J_{scale}/k_{f\ scale}$ increases slightly, from $1.35\pm0.14 \times (J/k_f)_{JPL06}$ (all data points) to $1.44\pm0.18 \times (J/k_f)_{JPL06}$ (8 and 9 September excluded), if $K_{eq} = K_{eq\ JPL06}$. The difference between the two calculations is not statistically significant. This result shows the sensitivity of the applied OE method to the a priori ClO_x information. Since there is no valid scientific reason for excluding these two days in question, and because they have only a small effect on the retrieved value of $J_{scale}/k_{f\ scale}$, these two days were retained in the prior results of this section as well as in the OE analyses discussed further in Sect. 5.

4.2 Exploring the full parameter space

In contrast to the OE approach, the $k_{f\ scale}$, J_{scale}, and $K_{eq\ scale}$ parameter space was explored to derive the optimal ClO dimer cycle kinetic parameters required to explain the measured ClO. The study by Santee et al. (2010) reported that SLIMCAT overestimates the ClO_x concentration by about 25% in the Antarctic. Since the ClO_x values obtained from SLIMCAT may be uncertain, sensitivity to ClO_x was also explored by scaling ClO_x from 0.5 to 1.0. Scalings above 1.0 were not considered since this resulted in ClO_x occasionally exceeding Cl_y. J_{scale} was varied between 0.1 and 2.5, while $k_{f\ scale}$ was varied between 0.4 and 1.6. An upper bound of $K_{eq\ scale} = 1.6$ was used since JPL09 and most other studies (with the notable exceptions of Nickolaisen et al.

(1994); Ferracci and Rowley (2010)) suggest $K_{eq\ scale} \leq 0.7$. Within this space, the kinetic values that give the smallest RMS of the difference between modelled and measured ClO were determined.

The results from exploring the full parameter space would be best represented in a 4-D plot. However, a 4-D plot is far too complex and impossible to show on 2-D paper and for the purpose of this study it is sufficient and necessary to display the results in two dimensions. From the number of available 2-D plots (i.e. 90 figures could be drawn showing the evolution of J and k_f with changing K_{eq} and ClO_x), 15 plots were generated where the minimum RMS values for every combination of J and k_f corresponding to one of the 6 ClO_x scalings were determined for every K_{eq} separately. The minimum RMS values (from the 6 ClO_x scalings) are shown for each combination of J_{scale} and $k_{f\ scale}$ and for a selected number of $K_{eq\ scale}$ ($K_{eq} = 0.4$, 0.8, 1.2 and 1.6) in Fig. 3. In all cases the lowest RMS values are found for $ClO_{x\ scale} = 1.0$ (unshaded regions in Fig. 3) and the absolute minimum RMS for the highest $K_{eq\ scale}$ (Fig. 3d), in agreement with the results obtained from OE. While lower RMS values might have been found for $ClO_{x\ scale} > 1.0$, this would be physically unrealistic for the reasons detailed above. The calculated minimum RMS in the J_{scale}-$k_{f\ scale}$ plane, for each $K_{eq\ scale}$, shows little dependence on $K_{eq\ scale}$, confirming again that our measurements do not provide a strong constraint on K_{eq}.

The RMS values define a "valley" of minima in each J_{scale}-$k_{f\ scale}$ plane. According to Eq. (1) a given ClO_x and observed ClO concentration constrain the $[ClO]^2/[ClOOCl]$ ratio and J_{scale} and $k_{f\ scale}$ must essentially increase or decrease together. This explains the orientation of the valley of minimum RMS values seen in Fig. 3. The angle that this valley makes with the X-axis decreases slightly with increasing $K_{eq\ scale}$, indicating a decrease in $J_{scale}/k_{f\ scale}$ with increasing $K_{eq\ scale}$, which is in agreement with the results from the 19 OE runs described in Sect. 4.1. The ClO measurements mostly give information on J/k_f and contain very little information on these parameters individually (see Sect. 3). Therefore, the J/k_f ratio that best explains the ClO measurements can be derived from the orientation of the valley with an uncertainty constrained by the width of the valley. For higher $K_{eq\ scale}$ values (panels b-d in Fig. 3), the orientation of the valley suggests a $J_{scale}/k_{f\ scale}$ ratio smaller than 1, which would disagree with the OE result. However, taking the absolute minimum RMS in each panel leads to $J_{scale}/k_{f\ scale}$ of $\sim$1.66 for $K_{eq\ scale} = 0.4$, 0.8, and 1.2, and $J_{scale}/k_{f\ scale} = 1.25$ for $K_{eq\ scale} = 1.6$ (at the absolute minimum RMS). This independently derived result is in good agreement with the retrieved ratios of 1.62 ± 0.24, 1.40 ± 0.16, 1.32 ± 0.13 and 1.27 ± 0.28 from OE, for $K_{eq\ scale}$ prescribed at 0.4, 0.8, 1.2, and 1.6, respectively. However, the resulting valley of RMS minima using $J_{scale}/k_{f\ scale}$ ratios of 1.66 and 1.25 would require $ClO_{x\ scale}$ values smaller than 1.

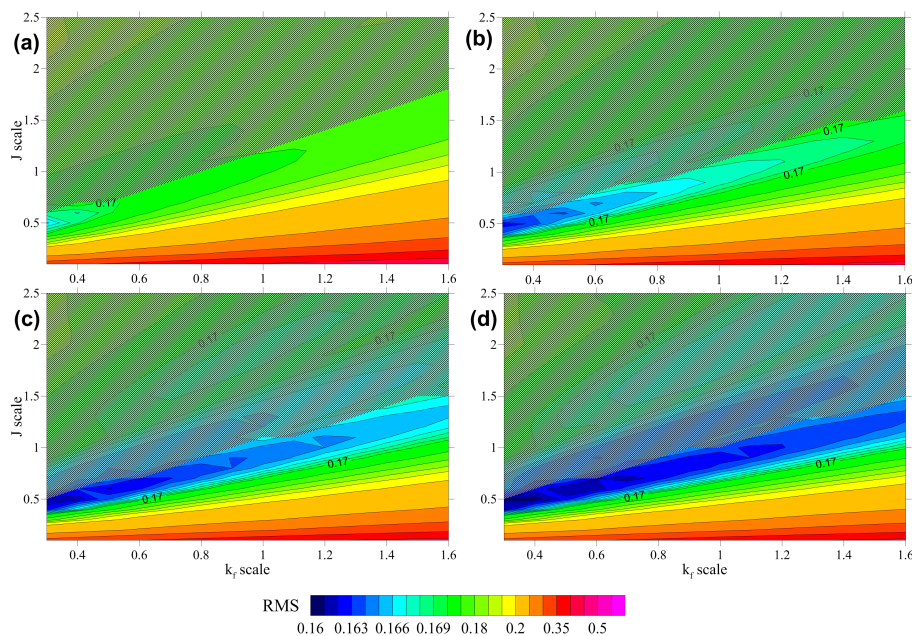**Fig. 3.** Scale factors for J and k_f with the corresponding RMS minimum derived from exploring the parameter space by varying $k_{f\,scale}$, J_{scale}, $K_{eq\,scale}$, and ClO$_x$ scale. The derived RMS minimum values are shown for prescribed $K_{eq\,scale}$ of 0.4 **(a)**, $K_{eq\,scale}$ of 0.8 **(b)**, $K_{eq\,scale}$ of 1.2 **(c)**, and $K_{eq\,scale}$ of 1.6 **(d)**. The blue colour scale indicates the smallest RMS values (below 0.168), while RMS values greater than 0.2 are shown in orange/red colours. The dark, hatched area towards the top left of the panels shows the RMS values where the ClO$_x$ scale factor was not equal to 1 (for details see text).

The RMS values obtained from exploring the whole parameter space are more than twice as large as those resulting from OE. Therefore, the results from the OE approach lead to a better fit to the ClO measurements than the results from exploring the whole parameter space. Contrary to the OE approach, the sampling of the whole parameter space does not readily permit changing the ClO$_x$ value from day to day or from one altitude level to another. The parameter space exploration scales ClO$_x$ values on all days and at all levels equally. This most likely explains the higher RMS values for the parameter space exploration.

5   Discussion

The retrieved kinetic parameters from the optimal estimation runs (Sect. 4.1) and the results derived by exploring the whole parameter space (Sect. 4.2) agree very well within the given uncertainties of optimal estimation. The retrieved $J_{scale}/k_{f\,scale}$ ratios for various $K_{eq\,scale}$ reflect a range of combinations of J, k_f, and K_{eq} values which are consistent with the Antarctic ClO measurements, i.e. there is not only one optimal combination of J, k_f, and K_{eq}. The possible combinations of kinetic parameters derived in previous field and laboratory studies and values recommended by JPL that can be used to explain the ClO observations are discussed below.

In agreement with Stimpfle et al. (2004), using a J_{JPL06} value together with a smaller k_f value relative to JPL06 (Trolier et al., 1990) was found to reproduce the ClO measurements. Furthermore, Stimpfle et al. concluded that the laboratory measurement of K_{eq} from Cox and Hayman (1988) agrees best with ClO and ClOOCl observations ($190\,\mathrm{K} < T < 200\,\mathrm{K}$). Prescribing the K_{eq} value derived by Cox and Hayman results in a $J_{scale}/k_{f\,scale}$ ratio of 1.54±0.21. This ratio would also include such a combination of J and k_f as mentioned above, i.e. J_{JPL06} and $k_{f\,Trolier}$, to explain the ClO measurements.

K_{eq} determined by Plenge et al. (2005) would lead to a J/k_f ratio of $1.75\pm0.51\times(J/k_f)_{JPL06}$. This result suggests that the photolysis frequency of the dimer is higher than currently recommended and lies within the range of 1.25 to $2.25 \times J_{JPL06}$ if $k_{f\,JPL06}$ is correct. If the photolysis frequency determined by JPL06 is used, then k_f has to be smaller than currently recommended (between 45 % and 80 % of $k_{f\,JPL06}$). These results suggest that using $K_{eq\,Plenge}$ would lead to higher modelled ClO abundances than using the current JPL recommendations.

If K_{eq} is fixed to JPL06 then our results indicate that $J/k_f = 1.35\pm0.14\times(J/k_f)_{JPL06}$. Using J_{JPL06} requires a smaller k_f value than currently recommended and our results show that k_f must lie in the range of 0.6 to $0.95\times k_{f\,JPL06}$ to explain the measurements. Therefore, the results presented by Bloss et al. (2001) and Trolier et al. (1990) for k_f together

with the JPL06 recommendation for J and K_{eq} are consistent with the ClO measurements used in this study.

Using a combination of $K_{eq\ scale} = 0.2$ (which is at the lowest end of the $K_{eq\ scale}$ range explored in this study) and a J value obtained from the Burkholder et al. (1990) cross-sections, which agrees with the value of J found using cross-sections of the more recent study by Papanastasiou et al. (2009), requires a $k_{f\ scale}$ value greater than 0.55 to be consistent with the ClO measurements. An increase in both J and k_f relative to the JPL06 recommendation would lead to an increase in the calculated ozone loss by the ClO dimer cycle, because chlorine is cycled more quickly through the different steps of the catalytic cycle.

Night-time ClO measurements were used in the past to determine the equilibrium constant (e.g., Stimpfle et al., 2004; von Hobe et al., 2005; Santee et al., 2010). Given these studies and studies performed in the laboratory (e.g., Plenge et al., 2005), it is more likely that $K_{eq\ scale}$ lies between 0.27 and 0.5 than being far greater than recommended by JPL06. Furthermore, the study by von Hobe et al. (2007) found that their stratospheric ClO observations were described well using a similar scaling for K_{eq}. The JPL09 recommendation also provides a smaller K_{eq} value ($0.7 \times K_{eq\ JPL06}$) than previously recommended in JPL06. The range of $K_{eq\ scale}$ between 0.27 and 0.7, together with the results from our OE approach, suggest that J/k_f values lie between 1.75 ± 0.29 and $1.44 \pm 0.17 \times (J/k_f)_{JPL06}$. The analyses presented above show that using these combinations of the kinetic parameters would include J and k_f values which are consistent with the JPL06 recommendations within the given uncertainty ranges of J_{JPL06} and $k_{f\ JPL06}$. Furthermore, this result would preclude J values smaller than currently recommended (e.g., Pope et al., 2007) and would exclude the lower uncertainty range on the J_{JPL06} value.

6 Summary and conclusions

Two methods, both using ground-based ClO measurements made during the period from 21 August to 20 September 2005 in Antarctica, to derive the key kinetic parameters that govern the day-time partitioning between ClO and ClOOCl were presented. The day-time ClO profiles were retrieved from day minus night spectra, where the measured night-time spectrum was subtracted from the measured day-time spectrum. As a result, the Antarctic ClO measurements mostly contain information about J/k_f, where J is the photolysis frequency and k_f the ClO dimer formation rate. This study aimed to deduce the best J/k_f ratio, representing the optimal fit to the measurements. Rather than working with the kinetic parameters explicitly, they are specified as scalings relative to JPL06 recommendations. The retrieved $J_{scale}/k_{f\ scale}$ ratio then provides a range of combinations of J_{scale} and $k_{f\ scale}$ that are consistent with the ClO measurements. Due to the day minus night subtraction performed in obtaining the mea-

sured ClO profile, no attempt was made to retrieve the equilibrium constant K_{eq}. Rather, to allow a sensitivity study of the derived $J_{scale}/k_{f\ scale}$ ratios to a choice of K_{eq}, K_{eq} was varied within physically plausible limits.

First, optimal estimation (OE) was applied to retrieve the optimal J/k_f ratio that corresponds to the minimum of the differences between measured and calculated ClO concentrations. Nineteen optimal estimation runs were performed where K_{eq} was prescribed to values between 0.2 and $2.0 \times K_{eq\ JPL06}$. To confirm the results from the optimal estimation, and to test how much more information can be derived when sampling the whole parameter space, one run was performed where the kinetic parameters and the ClO$_x$ profiles were varied within physically plausible ranges to determine the combination of these parameters that minimizes the sum of the squares of the differences between the modelled and the measured ClO profiles.

The results presented above confirm, as also shown in Schofield et al. (2008), that OE is a reliable method for investigating the kinetics of the ClO dimer cycle. The results derived by exploring the whole parameter space agree with the retrieved kinetics from the OE runs. OE has the advantage that it is much faster than sampling the parameter space and provides quantitative estimates of the uncertainties on the derived parameters. Furthermore, the OE retrieves a quantitative estimate of the daily ClO$_x$ abundances required to explain the observed ClO concentrations. Exploring the whole 4-D space is computationally expensive and changing ClO$_x$ individually for every day would make it even more so. OE gives one set of parameters and, as shown above, these results provide a reliable fit to the measurements.

The results presented above indicate that the retrieved $J_{scale}/k_{f\ scale}$ ratios from all 19 OE runs agree with most values reported in previous studies and lie within the lower half of the large uncertainty range reported by JPL06. The recently updated JPL09 recommendation reports a much smaller uncertainty range on the ClOOCl absorption cross-sections than JPL06. As a result, the uncertainty range on the ClOOCl photolysis frequency (J) is reduced, which in turn places tighter constraints on the J/k_f ratio than given by JPL06. The retrieved $J_{scale}/k_{f\ scale}$ for prescribed K_{eq} values of 0.4 to 1.2 times JPL06, which correspond to 0.6 to 1.7 times JPL09, lies within the upper part of the uncertainty range given for J/k_f by JPL09.

The 2005 ground-based microwave ClO measurements made over Scott Base, Antarctica, can be explained using the JPL06 recommendations of J, k_f, and K_{eq} with the given range of uncertainties (Fig. 2). Our study suggests a greater value of J/k_f than the JPL06 value (i.e., either faster photolysis of ClOOCl, slower rate of formation of ClOOCl by the self reaction of ClO, or some combination of these two perturbations), but the retrieved values lie within the rather large uncertainty limits of the JPL recommendations.

The best fit to the ClO measurements is achieved by using a higher $K_{eq\ scale}$ value ($K_{eq} = 2.0 \times K_{eq\ JPL06}$) than currently

recommended by JPL06/09, leading to a $J_{\text{scale}}/k_{\text{f scale}}$ value of $1.23 \pm 0.11 \times (J/k_f)_{\text{JPL06}}$. While this finding agrees with the higher K_{eq} values found by Ferracci and Rowley (2010), we caution that our retrieved values of K_{eq} are not well constrained by the measurements of ClO.

K_{eq} governs the partitioning of ClO and its dimer primarily during the night. Therefore, ClO day-time measurements are only weakly sensitive to K_{eq}, which likely explains the small change in the RMS values over the relatively large prescribed range of $K_{\text{eq scale}}$ (0.2 to 2.0). Night-time measurements of ClO are required to determine a reliable value of K_{eq}. Although this study does not provide a tight constraint on K_{eq}, the retrieved J/k_f obtained here is robust against the uncertainty in K_{eq}. However using both day-time and night-time measurements would provide a means to estimate K_{eq} and an estimate of J/k_f that would be largely independent of K_{eq}.

The results presented above are in basic agreement with earlier field and laboratory studies. In this study, a single value for J/k_f could not be determined due to the lack of night-time ClO observations, rather a range of J/k_f ratios was provided depending on what is assumed for K_{eq}. This highlights the need for a greater number of night-time ClO measurements under stratospheric conditions to derive independent information on the kinetic parameters governing the effectiveness of the ClO dimer cycle.

References

Atkinson, R., Baulch, D. L., Cox, R. A., Crowley, J. N., Hampson, R. F., Hynes, R. G., Jenkin, M. E., Rossi, M. J., and Troe, J.: Evaluated kinetic and photochemical data for atmospheric chemistry: Volume III – gas phase reactions of inorganic halogens, Atmos. Chem. Phys., 7, 981–1191, doi:10.5194/acp-7-981-2007, 2007.

Bloss, J. W., Nickolaisen, S. L., Salawitch, R. J., Friedl, R. R., and Sander, S. P.: Kinetics of the ClO self-reaction and 210 nm absorption cross section of the ClO dimer, J. Phys. Chem. A, 105, 11226–11239, 2001.

Burkholder, J. B., Orlando, J. J., and Howard, C. J.: Ultraviolet absorption cross sections of Cl_2O_2 between 210 and 410 nm, J. Phys. Chem., 94, 687–695, 1990.

Chen, H. Y., Lien, C.-Y., Lin, W.-Y., Lee, Y. T., and Lin, J. J.: UV Absorption Cross Section of ClOOCl Are Consistent With Ozone Degradation Models, Science, 324, 781–784, 2009.

Chipperfield, M. P.: Multiannual simulations with a three-dimensional chemical transport model, J. Geophys. Res., 104, 1781–1805, 1999.

Chipperfield, M. P.: New version of the TOMCAT/SLIMCAT offline chemical transport model: Intercomparison of stratospheric tracer experiments, Q. J. Roy. Meteorol. Soc., 132, 1179–1203, 2006.

Connor, B. J., Mooney, T., Barret, J. W., Solomon, P., Parrish, A., and Santee, M. L.: Comparison of ClO measurements from the Aura Microwave Limb Sounder to ground-based microwave measurements at Scott Base, Antarctica, in spring 2005, J. Geophys. Res., 112, D24S42, doi:10.1029/2007JD008792, 2007.

Cox, R. A. and Hayman, G. D.: The stability and photochemistry of dimers of the ClO radical and implications for Antarctic ozone depletion, Nature, 332, 796–800, 1988.

Feng, W., Chipperfield, M. P., Dorf, M., Pfeilsticker, K., and Ricaud, P.: Mid-latitude ozone changes: studies with a 3-D CTM forced by ERA-40 analyses, Atmos. Chem. Phys., 7, 2357–2369, doi:10.5194/acp-7-2357-2007, 2007.

Ferracci, V. and Rowley, D. M.: Kinetic and thermochemical studies of the ClO + ClO + M $\leftrightarrows$ Cl_2O_2 + M reaction, Phys. Chem. Chem. Phys., 12, 11596–11608, 2010.

Frieler, K., Rex, M., Salawitch, R. J., Canty, T., Streibel, M., Stimpfle, R. M., Pfeilsticker, K., Dorf, M., Weisenstein, D. K., and Godin-Beekmann, S.: Toward a better quantitative understanding of polar stratospheric ozone loss, Geophys. Res. Lett., 33, L10812, doi:10.1029/2005GL025466, 2006.

Hassler, B., Bodeker, G. E., and Dameris, M.: Technical Note: A new global database of trace gases and aerosols from multiple sources of high vertical resolution measurements, Atmos. Chem. Phys., 8, 5403–5421, doi:10.5194/acp-8-5403-2008, 2008.

Huder, K. J. and DeMore, W. B.: Absorption Cross Sections of the ClO Dimer, J. Phys. Chem., 99, 3905–3908, 1995.

Kalnay, E., Kanamitsu, M., Kistler, R., Collins, W., Deaven, D., Gandin, L., Iredell, M., Saha, S., White, G., Woollen, J., Zhu, Y., Chelliah, M., Ebisuzaki, W., Higgins, W., Janowiak, J., Mo, K. C., Ropelewski, C., Wang, J., Leetmaa, A., Reynolds, R., Jenne, R., and Joseph, D.: The NCEP/NCAR 40-year reanalysis project, B. Am. Meteorol. Soc., 77, 437–471, 1996.

Molina, L. T. and Molina, M. J.: Production of the Cl_2O_2 from the Self-Reaction of the ClO Radical, J. Phys. Chem., 91, 433–436, 1987.

Nickolaisen, S. L., Friedl, R. R., and Sander, S. P.: Kinetics and mechanism of the ClO-ClO reaction - pressure and temperature dependence of the bimolecular and termolecular channels and thermal-decomposition of chlorine peroxide, J. Phys. Chem., 98, 155–169, 1994.

Papanastasiou, D. K., Papadimitriou, V. C., Fahey, D. W., and Burkholder, J. B.: UV Absorption Spectrum of the ClO Dimer (Cl_2O_2) between 200 and 420 nm, J. Phys. Chem. A, 113, 13711–13726, 2009.

Plenge, J., Kuehl, S., Vogel, B., Müller, R., Stroh, F., von Hobe, M., Flesch, R., and Ruehl, E.: Bond Strength of Chlorine Peroxide, J. Phys. Chem. A, 109, 6730–6734, 2005.

Pope, F. D., Hansen, J. C., Bayes, K. D., Friedl, R. R., and Sander, S. P.: Ultraviolet absorption spectrum of chlorine peroxide, ClOOCl, J. Phys. Chem. A, 111, 4322–4332, 2007.

Rodgers, C. D.: Inverse Methods For Atmospheric Sounding: Theory and Practice, World Scientific Publishing Co. Pte. Ltd., 2, 240, 2000.

Salawitch, R. J., Wofsy, S. C., Gottlieb, E. W., Lait, L. R., Newman, P. A., Schoeberl, M. R., Loewenstein, M., Podolske, J. R., Strahan, S. E., Proffitt, M. H., Webster, C. R., May, R. D., Fahey, D. W., Baumgardner, D., Dye, J. E., Wilson, J. C., Kelly, K. K., Elkins, J. W., and Chan, K. R.: Chemical loss of ozone in the Arctic polar vortex in the winter of 1991–1992, Science, 261, 1146–1149, 1993.

Sander, S. P., Friedl, R. R., Golden, D. M., Kurylo, M. J., Huie, R. E., Orkin, V. L., Moortgat, G. K., Ravishankara, A. R., Kolb, C. E., Molina, M. J., and Finlayson-Pitts, B. J.: Chemical Kinetics and Photochemical Data for Use in Atmospheric Studies, Evaluation Number 14, JPL Publication 02–25, Jet Propulsion Laboratory, Pasadena, CA, USA, 2003.

Sander, S. P., Friedl, R. R., Golden, D. M., Kurylo, M. J., Moortgat, G. K., Keller-Rudek, H., Wine, P. H., Ravishankara, A. R., Kolb, C. E., Molina, M. J., Finlayson-Pitts, B. J., Huie, R. E., and Orkin, V. L.: Chemical Kinetics and Photochemical Data for Use in Atmospheric Studies, Evaluation Number 15, JPL Publication 06-02, Jet Propulsion Laboratory, 2006.

Sander, S. P., Finlayson-Pitts, B. J., Friedl, R. R., Golden, D. M., Huie, R. E., Keller-Rudek, H., Kolb, C. E., Kurylo, M. J., Molina, M. J., Moortgat, G. K., Orkin, V. L., Ravishankara, A. R., and Wine, P. H.: Chemical Kinetics and Photochemical Data for Use in Atmospheric Studies, JPL Publication 09-31, Jet Propulsion Laboratory (Interim update to JPL06), 2009.

Santee, M. L., Sander, S. P., Livesey, N. J., and Froidevaux, L.: Constraining the chlorine monoxide (ClO)/chlorine peroxide (ClOOCl) equilibrium constant from Aura Microwave Limb Sounder measurements of nighttime ClO, Proc. Natl. Acad. Sci. USA, 107, 6588–6593, 2010.

Schofield, R., Connor, B. J., Kreher, K., Johnston, P. V., and Rodgers, C. D.: The retrieval of profile and chemical information from ground-based UV-visible spectroscopic measurements, J. Quant. Spectrosc. Radiat. Transfer., 86, 115–131, 2004.

Schofield, R., Frieler, K., Wohltmann, I., Rex, M., von Hobe, M., Stroh, F., Koch, G., Peter, T., Canty, T., Salawitch, R., and Volk, C. M.: Polar Stratospheric Chlorine Kinetics from a Self-Match Flight during SOLVE-II/EUPLEX, Geophys. Res. Lett., 35, L01807, doi:10.1029/2007GL031,740, 2008.

Solomon, P. M., Barrett, J. W., Connor, B. J., Zoonematkermani, S., Parrish, A., Lee, A., Pyle, J., and Chipperfield, M.: Seasonal observations of chlorine monoxide in the stratosphere over Antarctica during the 1996–1998 ozone holes and comparison with SLIMCAT three-dimensional model, J. Geophys. Res., 105, 28979–29001, 2000.

Solomon, P. M., Connor, B. J., Barrett, J. W., Mooney, T., Lee, A., and Parrish, A.: Measurements of stratospheric ClO over Antarctica in 1996–2000 and implications for ClO dimer chemistry, Geophys. Res. Lett., 29(15), 1708, doi:10.1029/2002GL015232, 2002.

Solomon, P. M., Barrett, J. W., Mooney, T., Connor, B. J., Parrish, A., and Siskind, D. E.: Rise and decline of active chlorine in the stratosphere, Geophys. Res. Lett., 33, L18807, doi:10.1029/2006GL027029, 2006.

SPARC: The Role of Halogen Chemistry in Polar Stratospheric Ozone Depletion: Report from the June 2008 Cambridge, UK Workshop for an Initiative under the Stratospheric Processes and Their Role in Climate (SPARC) Project of the World Climate Research Programme, Tech. rep., printed No. 33, 2009.

Stimpfle, R. M., Wilmouth, D. M., Salawitch, R. J., and Anderson, J. G.: First measurements of ClOOCl in the stratosphere: The coupling of ClOOCl and ClO in the Arctic polar vortex, J. Geophys. Res., 109, D03301, doi:10.1029/2003JD003811, 2004.

Trolier, M., Mauldin III, R. L., and Ravishankara, A. R.: Rate coefficient for the termolecular channel of the self-reaction of ClO, J. Phys. Chem., 94, 4896–4907, 1990.

von Hobe, M., Grooß, J.-U., Müller, R., Hrechanyy, S., Winkler, U., and Stroh, F.: A re-evaluation of the ClO/Cl_2O_2 equilibrium constant based on stratospheric in-situ observations, Atmos. Chem. Phys., 5, 693–702, doi:10.5194/acp-5-693-2005, 2005.

von Hobe, M., Salawitch, R. J., Canty, T., Keller-Rudek, H., Moortgat, G. K., Grooss, J.-U., Müller, R., and Stroh, F.: Understanding the kinetics of the ClO dimer cycle, Atmos. Chem. Phys., 7, 3055–3069, doi:10.5194/acp-7-3055-2007, 2007.

von Hobe, M., Stroh, F., Beckers, H., Benter, T., and Willner, H.: The UV/Vis absorption spectrum of matrix-isolated dichlorine peroxide, ClOOCl, Phys. Chem. Chem. Phys., 11, 1571–1580, 2009.

Wilmouth, D. M., Hanisco, T. F., Stimpfle, R. M., and Anderson, J. G.: Chlorine-catalyzed ozone destruction: Cl atom production from ClOOCl photolysis, J. Phys. Chem. A, 113, 14099–14108, 2009.